

Constraints on Redshift-Binned Dark Energy using DESI BAO Data

Ye-Huang Pang,^{1,2,3,*} Xue Zhang,^{4,†} and Qing-Guo Huang^{1,2,3,‡}

¹*School of Fundamental Physics and Mathematical Sciences,*

Hangzhou Institute for Advanced Study, UCAS, Hangzhou 310024, China

²*School of Physical Sciences, University of Chinese Academy of Sciences, No. 19A Yuquan Road, Beijing 100049, China*

³*CAS Key Laboratory of Theoretical Physics, Institute of Theoretical Physics,
Chinese Academy of Sciences, Beijing 100190, China*

⁴*Center for Gravitation and Cosmology, College of Physical Science
and Technology, Yangzhou University, Yangzhou 225009, China*

We parameterize the equation of state of late-time dark energy as $w_{\text{bin}}(z)$, with three redshift bins, characterized by a constant equation of state in each bin. Then, we constrain the parameters of the $w_{\text{bin}}\text{CDM}$ model using datasets from DESI BAO data, *Planck* CMB power spectrum, ACT DR6 lensing power spectrum, and type Ia supernova distance-redshift data of Pantheon Plus/DES Y5/Union3. The significances for $w_1 > -1$ is 1.9σ , 2.6σ and 3.3σ , and w_2 is consistent with -1 within 1σ level, while 1.6σ , 1.5σ and 1.5σ for $w_3 < -1$ in these three data combinations with different choices of type Ia supernova datasets, respectively. Additionally, to alleviate H_0 tension, we incorporate the early dark energy (EDE) model in the early-time universe and add the SH0ES absolute magnitude M_b prior (or H_0 prior) to further constrain the $w_{\text{bin}}\text{EDE}$ model. In the $w_{\text{bin}}\text{EDE}$ model, we find a $w_{\text{bin}}(z)$ pattern similar to that in the $w_{\text{bin}}\text{CDM}$ model. The results of the three data combinations exhibit $w_1 > -1$ at 1.9σ , 1.7σ and 2.9σ level, meanwhile $w_3 < -1$ at 1.3σ , 1.3σ and 1.3σ level, respectively. In all, our results indicate that the transition of dark energy from phantom at high redshifts to quintessence at low redshifts is not conclusive.

I. INTRODUCTION

The accelerated expansion of the universe at the low redshift remains a mystery, awaiting to be uncovered through more preciser observations. Various astrophysical observations have been dedicated to tracking clues that can shed light on the evolution of dark energy evolution, particularly its equation of state (EoS). Observations of Type Ia supernovae (SN Ia) [1, 2] and large-scale structures [3, 4] could potentially illuminate the characteristics of dark energy.

The first-year cosmological results from DESI (Dark Energy Spectroscopy Instrument) have been released [5–7]. The results of the DESI 2024 BAO and their implications for dynamical dark energy continue to attract significant interest. In Ref. [7], the constraints of the $w_0w_a\text{CDM}$ model exhibit a deviation from the ΛCDM model by $2.5\sigma/3.5\sigma/3.9\sigma$, when using the data combination of CMB+DESI BAO+Pantheon Plus, CMB+DESI BAO+Union3 and CMB+DESI BAO+DES Y5, respectively. Concerns regarding the anomalous data points and identifying those that may contribute to the constrained dynamical behavior of dark energy has been discussed in Ref. [8, 9]. Numerous constraints on dark energy model reveal implications for different dark energy dynamics using the DESI data [10–17]. Model-independent reconstructions of dark energy evolution also provide insights directly from the data points through Gaussian process [18, 19] and crossing statistics [20]. Refer to recent relevant works in Ref. [21–30].

Furthermore, there have been some discussions about the consistency with other cosmological constraints [31–33]. The DESI data provide a new independent determination of the value of H_0 , and Ref. [34] found that combining DESI BAO with priors on $\Omega_m h^2$ and angular scale of sound horizon at recombination θ_* yields a value of $H_0 = 69.88 \pm 0.93$ km s⁻¹Mpc⁻¹, which is in tension with both *Planck* ($H_0 = 67.27 \pm 0.60$ km s⁻¹Mpc⁻¹) [35] and SH0ES measurements ($H_0 = 73.04 \pm 1.04$ km s⁻¹Mpc⁻¹) [36]. Various models aimed at alleviating the Hubble tension have also been constrained using the DESI data, including early dark energy (EDE) [37], varying electron mass [38], etc. It is argued that addressing both the H_0 tension and S_8 tension may involve late-time extensions, in addition to early-time new physics [39, 40]. Therefore, investigating constraints on late-time dark energy remains crucial for exploring cosmological concordance and assessing the feasibility of this hypothesis.

In this work, we employ a widely used parameterization for the dark energy EoS in the cosmological model [41–43], dividing redshifts into several bins with a constant EoS within each bin. Then, we utilize DESI BAO data and other observational data to constrain the cosmological parameters. Additionally, we incorporate the EDE model and apply

* pangyehuang22@mails.ucas.ac.cn

† corresponding author: zhangxue@yzu.edu.cn

‡ corresponding author: huangqg@itp.ac.cn

a binned parameterization for late-time dark energy to investigate the constraint results in this model, which is free from Hubble tension. This paper is organized as follows. In Sec. II, we present the binned parameterization of dark energy equation of state and its corresponding models. The data combinations and analysis methods are detailed in Sec. III. The results and related discussions are presented in Sec. IV. Finally, we conclude in Sec. V.

II. MODELS

In the late-time of the universe, in order to comprehend the evolution of EoS, we consider the w_{bin} dark energy. The redshift binned dark energy EoS parameterization in our study is artificially selected based on

$$w_{\text{bin}}(z) = \begin{cases} w_1, & 0 \leq z < 0.4 \\ w_2, & 0.4 \leq z < 0.8 \\ w_3, & 0.8 \leq z < 2.1 \\ -1, & z \geq 2.1 \end{cases} \quad (1)$$

The parameterization of dark energy EoS is non-continuous, with w_1, w_2 and w_3 being constant. In the redshift range $z > 2.1$, in light of insufficient data, we assume the Λ CDM model. The EoS constraint is primarily influenced by the data in the respective redshift bin, providing additional complementary results for probing the dark energy. We employ the w_{bin} dark energy in place of the cosmological constant in Λ CDM model, resulting a new model is referred to as $w_{\text{bin}}\text{CDM}$ model.

To alleviate the H_0 tension, in addition to the standard early-time cosmological evolution, we also consider the early dark energy model [44] combined with late-time dark energy described by $w_{\text{bin}}(z)$, which is labeled as the $w_{\text{bin}}\text{EDE}$ model. The early dark energy model introduces a scalar field ϕ with an axion-like potential,

$$V(\phi) = m^2 f^2 [1 - \cos(\phi/f)]^n, \quad (2)$$

which becomes activate around recombination. This reduces the sound horizon of recombination epoch and thus increases the inferred value of H_0 from the model fitting. Similar to the axion potential when $n = 1$, m represents the mass of the scalar field, and f is the axion decay constant. Generally, n is chosen to be 3. This scenario has been extensively discussed in previous research [45–48]. The parameters related to the EDE scalar field are $\{\log_{10} a_c, f_{\text{EDE}}, \phi_i\}$, where a_c corresponds to the scale factor when EDE reaches its maximum fractional energy density, f_{EDE} represents the fractional energy density of EDE at a_c , and ϕ_i denotes the initial value of the scalar field.

III. DATASETS AND METHODOLOGY

To constrain the $w_{\text{bin}}\text{CDM}$ model mentioned above, we employ a combination of CMB, DESI BAO, and SN datasets as in [7].

- The CMB data includes low- ℓ TT and EE power spectrum from *Planck*, the high- ℓ TTTEEE power spectrum from PR3 `plik` likelihood [49, 50], and the CMB lensing power spectrum from ACT DR4 [51].
- The DESI BAO data consists of 12 BAO samples obtained from observations on various tracers, including BGS ($z_{\text{eff}} = 0.30$), LRG ($z_{\text{eff}} = 0.51, 0.71$), ELG ($z_{\text{eff}} = 1.32$), LRG + ELG ($z_{\text{eff}} = 0.93$), quasar ($z_{\text{eff}} = 1.49$), and Ly α forest ($z_{\text{eff}} = 2.33$) [7].
- The SN data comprises non-calibrated supernova luminosity-distance measurements from Pantheon Plus ($0.001 < z < 2.26$) [2], Union3 [52], or DES Y5 ($0.025 < z < 1.3$) [53].

Due to the sampling prior volume effect [48, 54, 55], it is important to include the SH0ES H_0 prior when sampling the $w_{\text{bin}}\text{EDE}$ model. Regardless of the discussion on the biased H_0 posterior [45, 56], this H_0 prior is indeed necessary for new physics to alleviate the Hubble tension. Therefore, the data combination used to constrain $w_{\text{bin}}\text{EDE}$ model is CMB+DESI BAO+SN+SH0ES. When SN data is Pantheon Plus, we use a prior on supernova absolute magnitude M_b [36] instead of H_0 prior, and in this case, the results with these two priors are almost identical [57, 58]. We adopt flat prior on w_1, w_2 and w_3 over range $[-3, 1]$.

The cosmological parameter constraints is inferred through the chains of MCMC (Markov-chain Monte Carlo) sampling. We use the MCMC sampler of `cobaya` [59] and a modified version of `class` [46, 60]¹ to calculate observable

¹ The modified version of `class` for EDE can be assessed at <https://github.com/PoulinV/AxiCLASS>.

quantities. The MCMC chains are analysed using `getdist` [61]. To ensure convergence in our analysis, we require the Gelman-Rubin criterion [62] $R - 1 < 0.05$ for sampling process.

IV. RESULTS AND DISCUSSION

In Fig. 1, we present the mean value and the corresponding 1σ C.L. of w_i ($i = 1, 2, 3$) in each redshift bin inferred from MCMC chains. Fig. 2 shows the $w_1 - w_3$ plane in the $w_{\text{bin}}\text{CDM}$ and $w_{\text{bin}}\text{EDE}$ using different data combinations. The 2-dimensional posterior distribution of the $w_{\text{bin}}\text{CDM}$ and $w_{\text{bin}}\text{EDE}$ parameters is displayed in Fig. 3 and Fig. 4 respectively. Additionally, we list the mean values and 1σ C.L. of the $w_{\text{bin}}\text{CDM}$ and $w_{\text{bin}}\text{EDE}$ parameters, along with the χ^2 values for the best-fit parameters in Table I and Table II.

For the $w_{\text{bin}}\text{CDM}$ model, the EoS constraints in each redshift bin are $w_1 = -0.923 \pm 0.041$, $w_2 = -1.02 \pm 0.19$ and $w_3 = -1.62_{-0.25}^{+0.39}$ at 1σ C.L. when using data combination of CMB+BAO+Pantheon Plus. We find that, in this case, $w_1 > -1$ at $\sim 1.9\sigma$ level, w_2 is consistent with -1 within the 1σ level and $w_3 < -1$ at $\sim 1.6\sigma$ level. Although the mean w_3 value seems to deviate significantly from -1 , the large error bar diminishes the statistical significance of this deviation. As shown in Fig. 1, CMB+BAO+Union3 and CMB+BAO+DES Y5 yield similar w_{bin} constraints to the CMB+BAO+Pantheon Plus case, with slightly different mean values of w_i for $i = 1, 2, 3$. The significance of the tension with ΛCDM ($w = -1$) is 2.6σ and 3.3σ for w_1 , while 1.5σ and 1.5σ for w_3 in these two data combinations respectively. The detailed w_i mean values and corresponding 1σ confidence levels are listed in Table I. A comparison of the marginalized posterior distributions in $w_{\text{bin}}\text{CDM}$ model constrained by CMB+BAO+Pantheon Plus/Union3/DES Y5 can be seen in Fig. 3. We find that CMB+BAO+Pantheon Plus/Union3/DES Y5 constraints are compatible with each other.

Compared to the model-independent reconstruction of $w(z)$, such as the crossing statistics reconstruction [20], our results for w_{bin} can be interpreted as flattening out the evolution of $w(z)$ with respect to redshift, making it a constant value within each redshift bin. In Ref. [20], when reconstructed with CMB+BAO+Pantheon Plus/Union3/DES Y5 dataset, the redshift range $0 < z \lesssim 0.5$ exhibits $w > -1$, while the range $1.0 \lesssim z \lesssim 2.5$ shows $w < -1$ at $\gtrsim 1\sigma$ level. Therefore, it is not surprising that we observe our constrained results for w_{bin} , indicating that mean values of w_1 lie in quintessence regime and mean values of w_3 lie in phantom regime at $> 1\sigma$ level. However, due to the poor statistical significance, we cannot draw a simple conclusion about whether the data prefer the transition from phantom dark energy to quintessence. In the left panel of Fig. 2, we show the 2-dimensional (2D) marginalized posterior distributions in (w_1, w_3) plane. Since w_2 is consistent with -1 within the 1σ level, the (w_1, w_3) contours provide a visual method to determine whether dark energy evolves from the phantom regime in the third redshift bin to the quintessence regime in the first redshift bin. Specifically, if the (w_1, w_3) contour falls within the lower-right quadrant formed by the intersection of lines $w_1 = -1$ and $w_3 = -1$, it suggests that the dark energy EoS may exhibit phantom-like behavior at early times and be quintessence-like behavior at lower redshift. However, all of the (w_1, w_3) contours constrained by CMB+DES BAO+Pantheon Plus/Union3/DES Y5 intersect with line $w_3 = -1$, indicating that there is no significant preference for phantom dark energy at the third redshift bin.

For the $w_{\text{bin}}\text{EDE}$ model, the mean values and 1σ C.L. of EoS in each redshift bin are $w_1 = -0.925 \pm 0.040$, $w_2 = -1.10 \pm 0.18$ and $w_3 = -1.48_{-0.24}^{+0.37}$ when using data combination of CMB+BAO+Pantheon Plus+SH0ES. We

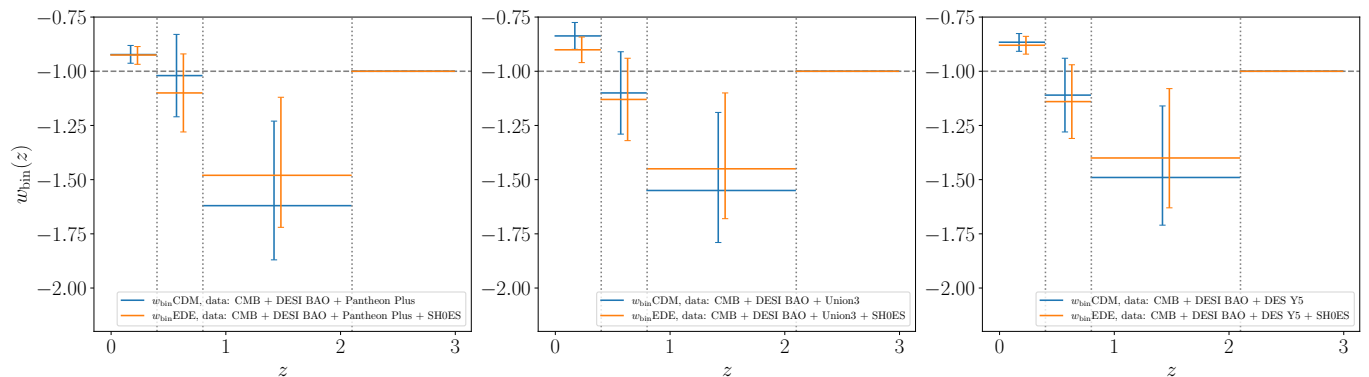


FIG. 1. The mean and 1σ confidence level (C.L.) of late-time dark energy EoS constraints with a combination of CMB + DESI BAO + SN data for the $w_{\text{bin}}\text{CDM}$ model (blue) and the $w_{\text{bin}}\text{EDE}$ model (orange). The SN data in the combined dataset correspond to Pantheon Plus, DES Y5, and Union3 from left to right. For clarity, we have offset the error bar plots of w_i , where $i = 1, 2, 3$.

find a similar trend, $w_1 > -1$ at $\sim 1.9\sigma$ level, w_2 is consistent with -1 within 1σ level, and $w_3 < -1$ at $\sim 1.3\sigma$ level. The corresponding constraints on w_{bin} from CMB+BAO+Union3+SH0ES and CMB+BAO+DES Y5+SH0ES are depicted in Fig. 1. The results of these data combinations exhibit slightly discrepancies with Λ CDM at 1.7σ and 2.9σ level for w_1 , meanwhile 1.3σ and 1.3σ level for w_3 respectively. The 2D marginalized posterior distributions of the w_{bin} EDE model, constrained by CMB+BAO+Pantheon Plus/Union3/DES Y5+SH0ES, are illustrated in Fig. 4. These constraints demonstrate mutual compatibility. Additionally, the (w_1, w_3) contours are plotted in the right panel of Fig. 2, and the corresponding results do not prominently exhibit phantom to quintessence transition.

The fit to CMB+BAO+Pantheon Plus+SH0ES data yields $H_0 = 71.79 \pm 0.86 \text{ km s}^{-1} \text{ Mpc}^{-1}$ within the framework of the w_{bin} EDE model, which is consistent with the SH0ES result of $H_0 = 73.04 \pm 1.04 \text{ km s}^{-1} \text{ Mpc}^{-1}$ at 1σ level. For the CMB+BAO+Union3+SH0ES data, the resulting value of $H_0 = 71.20 \pm 0.88 \text{ km s}^{-1} \text{ Mpc}^{-1}$ deviates by approximately $\sim 1.4\sigma$ from the SH0ES result. The combination of CMB+BAO+DES Y5+SH0ES data yields $H_0 = 71.08 \pm 0.85 \text{ km s}^{-1} \text{ Mpc}^{-1}$, which deviates from SH0ES by $\sim 1.5\sigma$. In the EDE model, an increase of H_0 is accompanied by higher values of n_s, ω_c , and an exacerbated S_8 tension compared to the Λ CDM model [48, 63, 64]. Similar relative changes in these parameters are found when comparing constraints on w_{bin} CDM parameters in Fig. 3 with those on w_{bin} EDE in Fig. 4. We find that early-time physics, tightly constrained by CMB data, subsequently impact constraints on w_{bin} within the w_{bin} EDE model through shifts in parameters such as $\{\log(10^{10} A_s), n_s, \Omega_b h^2, \Omega_c h^2, \tau_{\text{reio}}\}$.

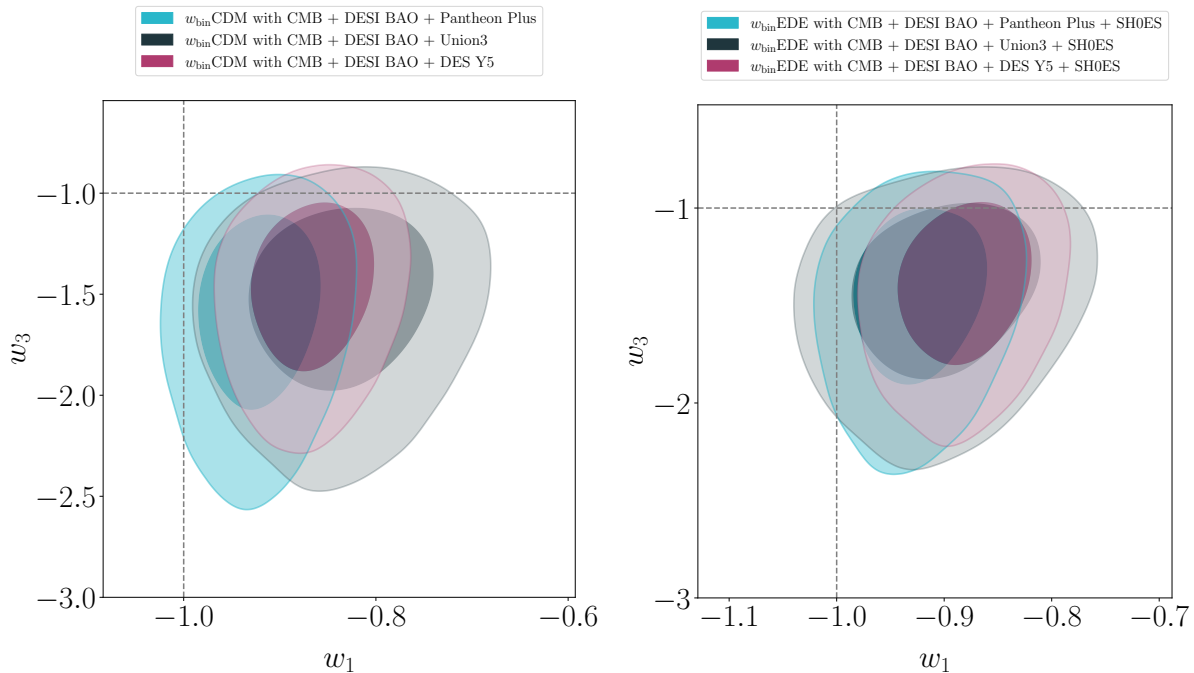


FIG. 2. Marginalized posterior distributions for w_1 and w_3 in the w_{bin} CDM model (left panel) and w_{bin} EDE model (right panel).

	CMB+BAO+Pantheon Plus	CMB+BAO+Union3	CMB+BAO+DES Y5
$\log(10^{10} A_s)$	$3.042(3.041) \pm 0.014$	$3.043(3.041) \pm 0.014$	$3.044(3.043) \pm 0.014$
n_s	$0.9640(0.9634) \pm 0.0040$	$0.9643(0.9634) \pm 0.0040$	$0.9645(0.9654) \pm 0.0040$
$H_0[\text{km s}^{-1}\text{Mpc}^{-1}]$	$68.24(67.995) \pm 0.74$	$67.12(67.06) \pm 0.95$	$67.51(67.36) \pm 0.69$
$\Omega_b h^2$	$0.02233(0.02228) \pm 0.00014$	$0.02234(0.02240) \pm 0.00014$	$0.02234(0.02236) \pm 0.00014$
$\Omega_c h^2$	$0.1203(0.1206) \pm 0.0011$	$0.1202(0.1203) \pm 0.0011$	$0.1202(0.1200) \pm 0.0011$
τ_{reio}	$0.0532(0.0525) \pm 0.0075$	$0.0537(0.0524) \pm 0.0074$	$0.0538(0.0527) \pm 0.0075$
w_1	$-0.923(-0.924) \pm 0.041$	$-0.837(-0.827) \pm 0.062$	$-0.866(-0.864) \pm 0.041$
w_2	$-1.02(-1.04) \pm 0.19$	$-1.10(-1.14) \pm 0.19$	$-1.11(-1.11) \pm 0.17$
w_3	$-1.62(-1.49)^{+0.39}_{-0.25}$	$-1.55(-1.46)^{+0.36}_{-0.24}$	$-1.49(-1.40)^{+0.33}_{-0.22}$
S_8	$0.836(0.839) \pm 0.011$	$0.839(0.838) \pm 0.011$	$0.837(0.836) \pm 0.011$
χ^2_{CMB}	1015.15	1015.22	1015.01
χ^2_{SN}	1402.26	22.87	1639.31
$\chi^2_{\text{DES I BAO}}$	12.57	11.52	11.64
χ^2_{bestfit}	2429.98	1049.61	2665.96

TABLE I. The mean (best-fit) and $\pm 1\sigma$ C.L. of the w_{bin} CDM model parameters are shown in the table, along with the corresponding χ^2 values for the best-fit parameters.

	CMB+BAO+Pantheon Plus+SH0ES	CMB+BAO+Union3+SH0ES	CMB+BAO+DES Y5+SH0ES
$\log(10^{10} A_s)$	$3.058(3.066) \pm 0.016$	$3.057(3.064) \pm 0.016$	$3.059(3.074) \pm 0.015$
n_s	$0.9827(0.9860) \pm 0.0080$	$0.9818(0.9872) \pm 0.0085$	$0.9836(0.9895) \pm 0.0080$
$H_0[\text{km s}^{-1}\text{Mpc}^{-1}]$	$71.79(72.21) \pm 0.86$	$71.20(71.60) \pm 0.88$	$71.08(71.70) \pm 0.85$
$\Omega_b h^2$	$0.02272(0.02264) \pm 0.00022$	$0.02272(0.02269) \pm 0.00023$	$0.02274(0.02281) \pm 0.00023$
$\Omega_c h^2$	$0.1300(0.1335) \pm 0.0035$	$0.1294(0.1329) \pm 0.0037$	$0.1302(0.1333) \pm 0.0036$
τ_{reio}	$0.0536(0.0549) \pm 0.0078$	$0.0537(0.0558) \pm 0.0078$	$0.0542(0.0595) \pm 0.0077$
f_{EDE}	$0.096(0.127) \pm 0.032$	$0.090(0.125) \pm 0.034$	$0.099(1.312) \pm 0.033$
$\log_{10} a_c$	$-3.61(-3.56)^{+0.15}_{-0.033}$	$-3.61(-3.57)^{+0.18}_{-0.035}$	$-3.60(-3.58)^{+0.14}_{-0.037}$
w_1	$-0.925(-0.914) \pm 0.040$	$-0.901(-0.857) \pm 0.058$	$-0.880(-0.878) \pm 0.041$
w_2	$-1.10(-1.18) \pm 0.18$	$-1.13(-1.20) \pm 0.19$	$-1.14(-1.14) \pm 0.17$
w_3	$-1.48(-1.20)^{+0.37}_{-0.24}$	$-1.45(-1.26)^{+0.35}_{-0.23}$	$-1.40(-1.20)^{+0.32}_{-0.22}$
S_8	$0.847(0.853) \pm 0.012$	$0.847(0.851) \pm 0.013$	$0.849(0.853) \pm 0.012$
χ^2_{CMB}	1014.45	1013.83	1015.42
$\chi^2_{\text{SN}+M_b}$	1454.12	-	-
χ^2_{SN}	-	23.50	1639.77
$\chi^2_{\text{DES I BAO}}$	12.31	12.37	11.79
χ^2_{bestfit}	2480.88	1053.53	2670.55

TABLE II. The mean (best-fit) and $\pm 1\sigma$ C.L. of w_{bin} EDE model parameters are presented. The table also includes the χ^2 values corresponding to the best-fit parameters.

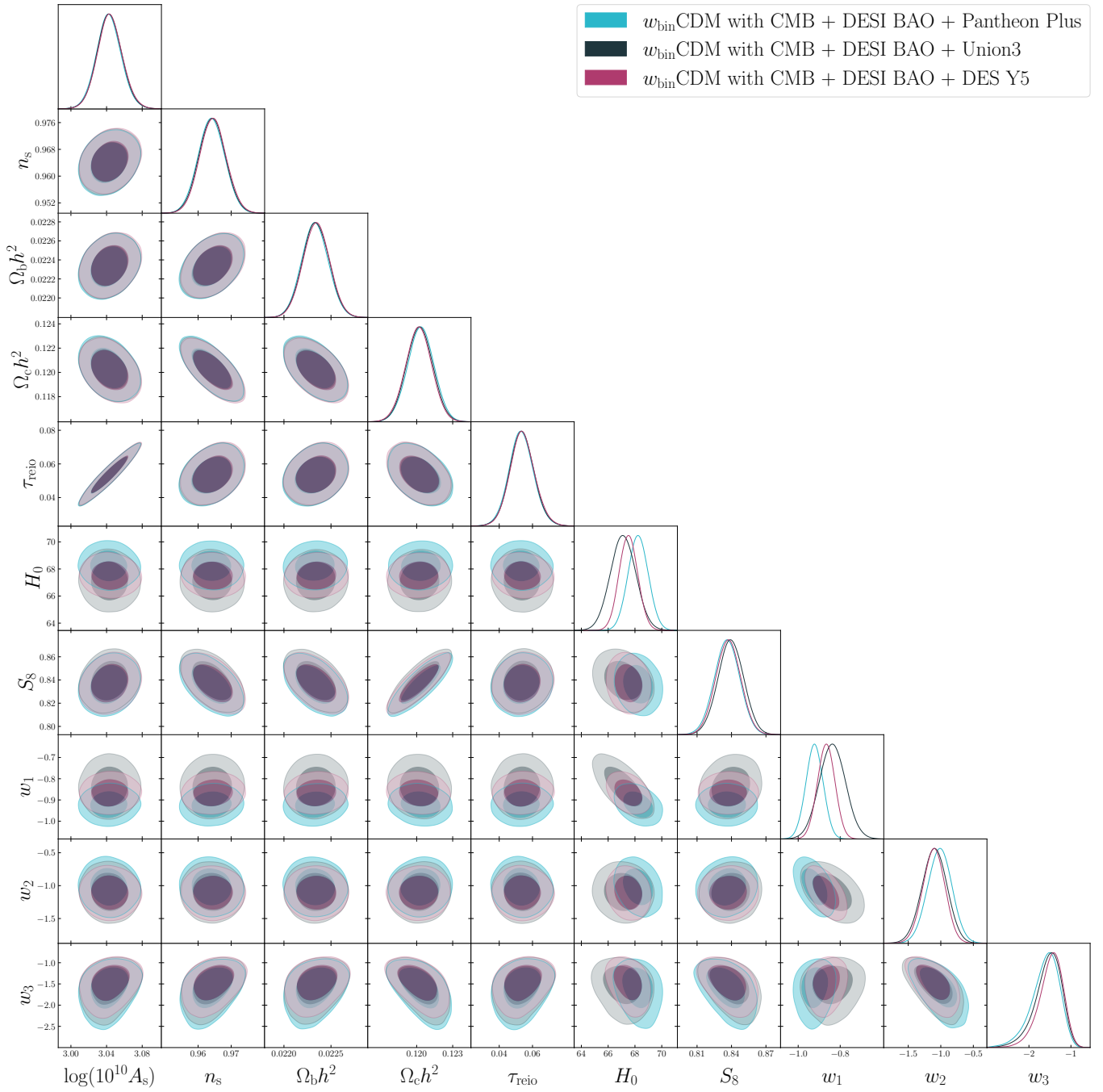


FIG. 3. The 2D posterior distribution of the $w_{\text{bin}}\text{CDM}$ model is presented at 1σ and 2σ C.L. The parameters are constrained using a combination of CMB + DESI BAO + Pantheon Plus/Union3/DES Y5 data.

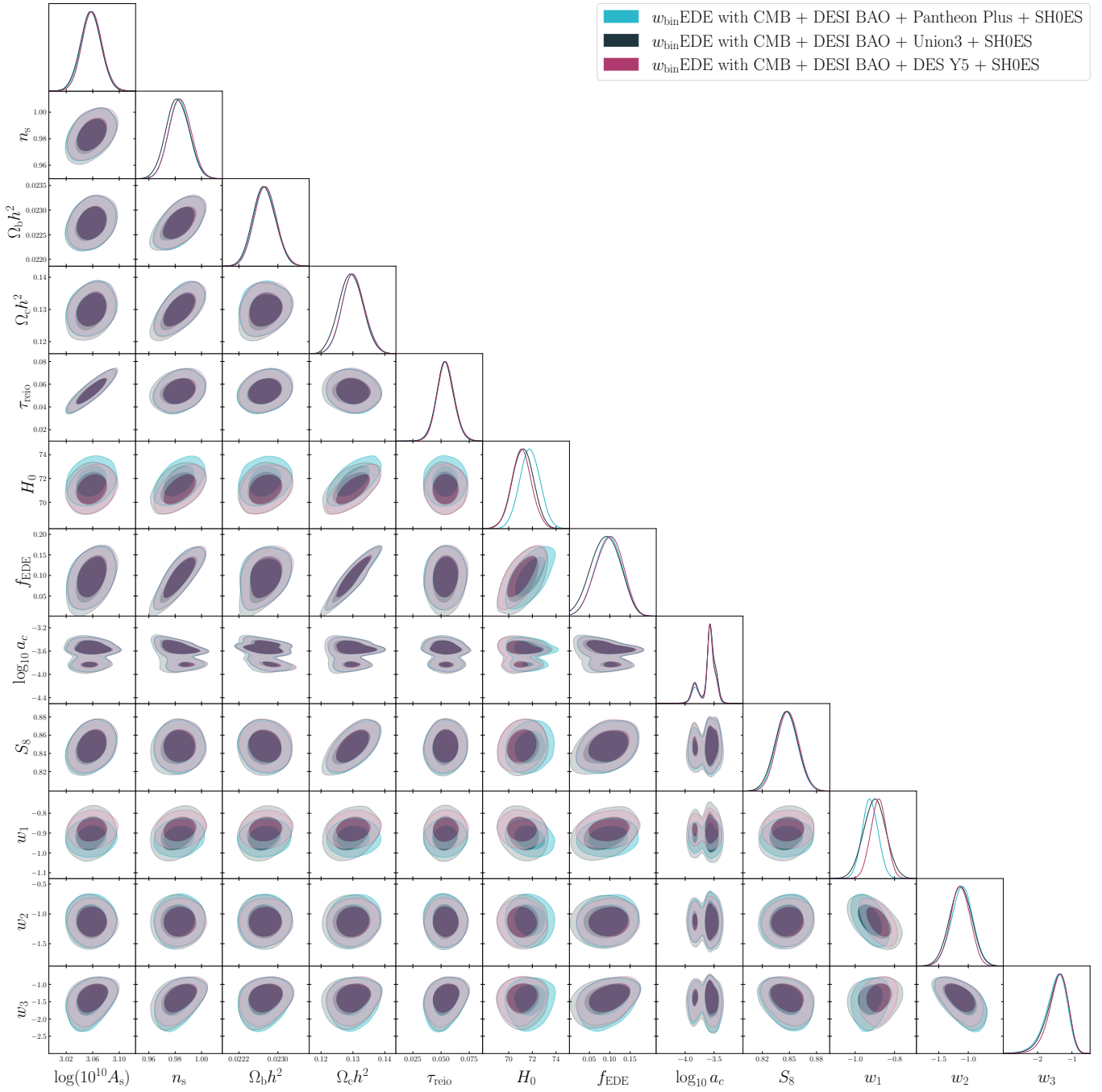


FIG. 4. The 2D posterior distribution of the $w_{\text{bin}}\text{EDE}$ model is shown at 1σ and 2σ C.L. The parameter constraints are derived from a combination of CMB + DESI BAO + Pantheon Plus/Union3/DES Y5 + SH0ES data.

V. SUMMARY AND CONCLUSIONS

In this paper, we examine the constraints on dark energy models using DESI 2024 BAO data and other cosmological dataset. We assume that the dark energy equation of state is constant in three redshift bins, with the equation of state being varied separately in each bin. We constrain the w_{bin} CDM model and w_{bin} EDE model using the *Planck* CMB power spectrum, ACT lensing power spectrum, DESI BAO data, and Pantheon Plus / DES Y5 / Union3 data. Furthermore, we incorporate SH0ES prior into the combined datasets when sampling the w_{bin} EDE model.

For the w_{bin} CDM model, in the first redshift bin ($0 \leq z < 0.4$), the mean value of w_{bin} , denoted as w_1 , is greater than -1 and deviates from Λ CDM at 1.9σ , 2.6σ and 3.3σ level. In the second redshift bin ($0.4 \leq z < 0.8$), w_2 is consistent with -1 within 1σ level. In the third redshift bin ($0.8 \leq z < 2.1$), the mean value of w_3 less than -1 and deviates from -1 at 1.6σ , 1.5σ and 1.5σ level. In addition to the $< 2\sigma$ deviation from cosmological constant-like EoS in the third redshift bin, our contour plots for (w_1, w_3) show limited significance for early phantom-like dark energy behaviour. Both the w_{bin} CDM model and the w_{bin} EDE model exhibit this characteristic when analyzed with their respective data combinations. Although the mean values of w_i between the two models are dissimilar to some extent, they remain consistent within 1σ . The observed variation in w_i may be attributed to shifted model parameter values in the w_{bin} EDE model compared to those in the w_{bin} CDM model, as well as to distinct SN datasets employed in our analysis. The incorporation of the w_{bin} parameterization into the EDE model does not compromise its ability to alleviate the H_0 tension. The resulting constraints on H_0 , using CMB + DESI BAO + Pantheon Plus + SH0ES, are consistent with SH0ES measurements within 1σ level. For both the combinations of CMB + DESI BAO + Union3 + SH0ES and CMB + DESI BAO + DES Y5 + SH0ES, these tensions are at $< 2\sigma$ confidence level.

Acknowledgements. We acknowledge the use of HPC Cluster of ITP-CAS. XZ is supported by grant from NSFC (Grant No. 12005183). QGH is supported by the grants from NSFC (Grant No. 12475065, 11991052), Key Research Program of Frontier Sciences, CAS, Grant No. ZDBS-LY-7009, and China Manned Space Program through its Space Application System.

-
- [1] D. M. Scolnic *et al.* (Pan-STARRS1), “The Complete Light-curve Sample of Spectroscopically Confirmed SNe Ia from Pan-STARRS1 and Cosmological Constraints from the Combined Pantheon Sample,” *Astrophys. J.* **859**, 101 (2018), [arXiv:1710.00845 \[astro-ph.CO\]](#).
 - [2] Dillon Brout *et al.*, “The Pantheon+ Analysis: Cosmological Constraints,” *Astrophys. J.* **938**, 110 (2022), [arXiv:2202.04077 \[astro-ph.CO\]](#).
 - [3] Ashley J. Ross, Lado Samushia, Cullan Howlett, Will J. Percival, Angela Burden, and Marc Manera, “The clustering of the SDSS DR7 main Galaxy sample – I. A 4 per cent distance measure at $z = 0.15$,” *Mon. Not. Roy. Astron. Soc.* **449**, 835–847 (2015), [arXiv:1409.3242 \[astro-ph.CO\]](#).
 - [4] Shadab Alam *et al.* (BOSS), “The clustering of galaxies in the completed SDSS-III Baryon Oscillation Spectroscopic Survey: cosmological analysis of the DR12 galaxy sample,” *Mon. Not. Roy. Astron. Soc.* **470**, 2617–2652 (2017), [arXiv:1607.03155 \[astro-ph.CO\]](#).
 - [5] A. G. Adame *et al.* (DESI), “DESI 2024 III: Baryon Acoustic Oscillations from Galaxies and Quasars,” (2024), [arXiv:2404.03000 \[astro-ph.CO\]](#).
 - [6] A. G. Adame *et al.* (DESI), “DESI 2024 IV: Baryon Acoustic Oscillations from the Lyman Alpha Forest,” (2024), [arXiv:2404.03001 \[astro-ph.CO\]](#).
 - [7] A. G. Adame *et al.* (DESI), “DESI 2024 VI: Cosmological Constraints from the Measurements of Baryon Acoustic Oscillations,” (2024), [arXiv:2404.03002 \[astro-ph.CO\]](#).
 - [8] Eoin Ó. Colgáin, Maria Giovanna Dainotti, Salvatore Capozziello, Saeed Pourojaghi, M. M. Sheikh-Jabbari, and Dejan Stojkovic, “Does DESI 2024 Confirm Λ CDM?” (2024), [arXiv:2404.08633 \[astro-ph.CO\]](#).
 - [9] Zhengyi Wang, Shijie Lin, Zhejie Ding, and Bin Hu, “The role of LRG1 and LRG2’s monopole in inferring the DESI 2024 BAO cosmology,” (2024), [arXiv:2405.02168 \[astro-ph.CO\]](#).
 - [10] Yuichiro Tada and Takahiro Terada, “Quintessential interpretation of the evolving dark energy in light of DESI,” (2024), [arXiv:2404.05722 \[astro-ph.CO\]](#).
 - [11] Kim V. Berghaus, Joshua A. Kable, and Vivian Miranda, “Quantifying Scalar Field Dynamics with DESI 2024 Y1 BAO measurements,” (2024), [arXiv:2404.14341 \[astro-ph.CO\]](#).
 - [12] David Shlivko and Paul Steinhardt, “Assessing observational constraints on dark energy,” (2024), [arXiv:2405.03933 \[astro-ph.CO\]](#).
 - [13] Sukannya Bhattacharya, Giulia Borghetto, Ameet Malhotra, Susha Parameswaran, Gianmassimo Tasinato, and Ivonne Zavala, “Cosmological constraints on curved quintessence,” (2024), [arXiv:2405.17396 \[astro-ph.CO\]](#).
 - [14] Omar F. Ramadan, Jeremy Sakstein, and David Rubin, “DESI Constraints on Exponential Quintessence,” (2024), [arXiv:2405.18747 \[astro-ph.CO\]](#).
 - [15] William Giarè, Miguel A. Sabogal, Rafael C. Nunes, and Eleonora Di Valentino, “Interacting Dark Energy after DESI Baryon Acoustic Oscillation measurements,” (2024), [arXiv:2404.15232 \[astro-ph.CO\]](#).

- [16] Celia Escamilla-Rivera and Rodrigo Sandoval-Orozco, “f(T) gravity after DESI Baryon acoustic oscillation and DES supernovae 2024 data,” *JHEAp* **42**, 217–221 (2024), [arXiv:2405.00608 \[astro-ph.CO\]](#).
- [17] Ioannis D. Gialamas, Gert Hütsi, Kristjan Kannike, Antonio Racioppi, Martti Raidal, Martin Vasar, and Hardi Veermäe, “Interpreting DESI 2024 BAO: late-time dynamical dark energy or a local effect?” (2024), [arXiv:2406.07533 \[astro-ph.CO\]](#).
- [18] Yuhang Yang, Xin Ren, Qingqing Wang, Zhiyu Lu, Dongdong Zhang, Yi-Fu Cai, and Emmanuel N. Saridakis, “Quintom cosmology and modified gravity after DESI 2024,” (2024), [arXiv:2404.19437 \[astro-ph.CO\]](#).
- [19] Purba Mukherjee and Anjan Ananda Sen, “Model-independent cosmological inference post DESI DR1 BAO measurements,” (2024), [arXiv:2405.19178 \[astro-ph.CO\]](#).
- [20] R. Calderon *et al.* (DESI), “DESI 2024: Reconstructing Dark Energy using Crossing Statistics with DESI DR1 BAO data,” (2024), [arXiv:2405.04216 \[astro-ph.CO\]](#).
- [21] Guo-Hong Du, Peng-Ju Wu, Tian-Nuo Li, and Xin Zhang, “Impacts of dark energy on weighing neutrinos after DESI BAO,” (2024), [arXiv:2407.15640 \[astro-ph.CO\]](#).
- [22] Gen Ye, Matteo Martinelli, Bin Hu, and Alessandra Silvestri, “Non-minimally coupled gravity as a physically viable fit to DESI 2024 BAO,” (2024), [arXiv:2407.15832 \[astro-ph.CO\]](#).
- [23] Tian-Nuo Li, Peng-Ju Wu, Guo-Hong Du, Shang-Jie Jin, Hai-Li Li, Jing-Fei Zhang, and Xin Zhang, “Constraints on interacting dark energy models from the DESI BAO and DES supernovae data,” (2024), [arXiv:2407.14934 \[astro-ph.CO\]](#).
- [24] Hao Wang, Gen Ye, and Yun-Song Piao, “Impact of evolving dark energy on the search for primordial gravitational waves,” (2024), [arXiv:2407.11263 \[astro-ph.CO\]](#).
- [25] Guanlin Liu, Yu Wang, and Wen Zhao, “Impact of LRG1 and LRG2 in DESI 2024 BAO data on dark energy evolution,” (2024), [arXiv:2407.04385 \[astro-ph.CO\]](#).
- [26] Tonghua Liu, Shuo Cao, and Jieci Wang, “A model-independent determination of the sound horizon using recent BAO measurements and strong lensing systems,” (2024), [arXiv:2406.18298 \[astro-ph.CO\]](#).
- [27] Hao Wang, Ze-Yu Peng, and Yun-Song Piao, “Can recent DESI BAO measurements accommodate a negative cosmological constant?” (2024), [arXiv:2406.03395 \[astro-ph.CO\]](#).
- [28] Junchao Wang, Zhiqi Huang, Yanhong Yao, Jianqi Liu, Lu Huang, and Yan Su, “A PAGE-like Unified Dark Fluid Model,” (2024), [arXiv:2405.05798 \[astro-ph.CO\]](#).
- [29] Zhiqi Huang *et al.*, “MEET-U Project I: The key drivers of the preference for dynamic dark energy,” (2024), [arXiv:2405.03983 \[astro-ph.CO\]](#).
- [30] Gan Gu, Xiaoma Wang, Xiaoyong Mu, Shuo Yuan, and Gong-Bo Zhao, “Dynamical Dark Energy in Light of Cosmic Distance Measurements. I. A Demonstration Using Simulated Datasets,” *Res. Astron. Astrophys.* **24**, 065001 (2024), [arXiv:2404.06303 \[astro-ph.CO\]](#).
- [31] Dimitrios Bousis and Leandros Perivolaropoulos, “Hubble tension tomography: BAO vs SnIa distance tension,” (2024), [arXiv:2405.07039 \[astro-ph.CO\]](#).
- [32] X. D. Jia, J. P. Hu, and F. Y. Wang, “Uncorrelated estimations of H_0 redshift evolution from DESI baryon acoustic oscillation observations,” (2024), [arXiv:2406.02019 \[astro-ph.CO\]](#).
- [33] R. Camilleri *et al.* (DES), “The Dark Energy Survey Supernova Program: An updated measurement of the Hubble constant using the Inverse Distance Ladder,” (2024), [arXiv:2406.05049 \[astro-ph.CO\]](#).
- [34] Levon Pogosian, Gong-Bo Zhao, and Karsten Jedamzik, “A consistency test of the cosmological model at the epoch of recombination using DESI BAO and Planck measurements,” (2024), [arXiv:2405.20306 \[astro-ph.CO\]](#).
- [35] N. Aghanim *et al.* (Planck), “Planck 2018 results. VI. Cosmological parameters,” *Astron. Astrophys.* **641**, A6 (2020), [Erratum: *Astron. Astrophys.* 652, C4 (2021)], [arXiv:1807.06209 \[astro-ph.CO\]](#).
- [36] Adam G. Riess *et al.*, “A Comprehensive Measurement of the Local Value of the Hubble Constant with 1 km s⁻¹ Mpc⁻¹ Uncertainty from the Hubble Space Telescope and the SH0ES Team,” *Astrophys. J. Lett.* **934**, L7 (2022), [arXiv:2112.04510 \[astro-ph.CO\]](#).
- [37] Hao Wang and Yun-Song Piao, “Dark energy in light of recent DESI BAO and Hubble tension,” (2024), [arXiv:2404.18579 \[astro-ph.CO\]](#).
- [38] Osamu Seto and Yo Toda, “DESI constraints on varying electron mass model and axion-like early dark energy,” (2024), [arXiv:2405.11869 \[astro-ph.CO\]](#).
- [39] João Rebouças, Jonathan Gordon, Diogo H. F. de Souza, Kunhao Zhong, Vivian Miranda, Rogerio Rosenfeld, Tim Eifler, and Elisabeth Krause, “Early dark energy constraints with late-time expansion marginalization,” *JCAP* **02**, 042 (2024), [arXiv:2302.07333 \[astro-ph.CO\]](#).
- [40] Sunny Vagnozzi, “Seven Hints That Early-Time New Physics Alone Is Not Sufficient to Solve the Hubble Tension,” *Universe* **9**, 393 (2023), [arXiv:2308.16628 \[astro-ph.CO\]](#).
- [41] M. Kowalski *et al.* (Supernova Cosmology Project), “Improved Cosmological Constraints from New, Old and Combined Supernova Datasets,” *Astrophys. J.* **686**, 749–778 (2008), [arXiv:0804.4142 \[astro-ph\]](#).
- [42] Qing-Guo Huang, Miao Li, Xiao-Dong Li, and Shuang Wang, “Fitting the constitution type Ia supernova data with the redshift-binned parametrization method,” *Phys. Rev. D* **80**, 083515 (2009), [arXiv:0905.0797 \[astro-ph.CO\]](#).
- [43] Qing-Guo Huang and Ke Wang, “How the dark energy can reconcile Planck with local determination of the Hubble constant,” *Eur. Phys. J. C* **76**, 506 (2016), [arXiv:1606.05965 \[astro-ph.CO\]](#).
- [44] Vivian Poulin, Tristan L. Smith, Tanvi Karwal, and Marc Kamionkowski, “Early Dark Energy Can Resolve The Hubble Tension,” *Phys. Rev. Lett.* **122**, 221301 (2019), [arXiv:1811.04083 \[astro-ph.CO\]](#).
- [45] J. Colin Hill, Evan McDonough, Michael W. Toomey, and Stephon Alexander, “Early dark energy does not restore cosmological concordance,” *Phys. Rev. D* **102**, 043507 (2020), [arXiv:2003.07355 \[astro-ph.CO\]](#).
- [46] Riccardo Murgia, Guillermo F. Abellán, and Vivian Poulin, “Early dark energy resolution to the Hubble tension in light

- of weak lensing surveys and lensing anomalies,” *Phys. Rev. D* **103**, 063502 (2021), [arXiv:2009.10733 \[astro-ph.CO\]](#).
- [47] Mikhail M. Ivanov, Evan McDonough, J. Colin Hill, Marko Simonović, Michael W. Toomey, Stephon Alexander, and Matias Zaldarriaga, “Constraining Early Dark Energy with Large-Scale Structure,” *Phys. Rev. D* **102**, 103502 (2020), [arXiv:2006.11235 \[astro-ph.CO\]](#).
- [48] Vivian Poulin, Tristan L. Smith, and Tanvi Karwal, “The Ups and Downs of Early Dark Energy solutions to the Hubble tension: a review of models, hints and constraints circa 2023,” (2023), [arXiv:2302.09032 \[astro-ph.CO\]](#).
- [49] N. Aghanim *et al.* (Planck), “Planck 2018 results. VIII. Gravitational lensing,” *Astron. Astrophys.* **641**, A8 (2020), [arXiv:1807.06210 \[astro-ph.CO\]](#).
- [50] N. Aghanim *et al.* (Planck), “Planck 2018 results. V. CMB power spectra and likelihoods,” *Astron. Astrophys.* **641**, A5 (2020), [arXiv:1907.12875 \[astro-ph.CO\]](#).
- [51] Frank J. Qu *et al.* (ACT), “The Atacama Cosmology Telescope: A Measurement of the DR6 CMB Lensing Power Spectrum and Its Implications for Structure Growth,” *Astrophys. J.* **962**, 112 (2024), [arXiv:2304.05202 \[astro-ph.CO\]](#).
- [52] David Rubin *et al.*, “Union Through UNITY: Cosmology with 2,000 SNe Using a Unified Bayesian Framework,” (2023), [arXiv:2311.12098 \[astro-ph.CO\]](#).
- [53] T. M. C. Abbott *et al.* (DES), “The Dark Energy Survey: Cosmology Results With ~ 1500 New High-redshift Type Ia Supernovae Using The Full 5-year Dataset,” (2024), [arXiv:2401.02929 \[astro-ph.CO\]](#).
- [54] Laura Herold, Elisa G. M. Ferreira, and Eiichiro Komatsu, “New Constraint on Early Dark Energy from Planck and BOSS Data Using the Profile Likelihood,” *Astrophys. J. Lett.* **929**, L16 (2022), [arXiv:2112.12140 \[astro-ph.CO\]](#).
- [55] George Efstathiou, Erik Rosenberg, and Vivian Poulin, “Improved Planck Constraints on Axionlike Early Dark Energy as a Resolution of the Hubble Tension,” *Phys. Rev. Lett.* **132**, 221002 (2024), [arXiv:2311.00524 \[astro-ph.CO\]](#).
- [56] Eleonora Di Valentino, Olga Mena, Supriya Pan, Luca Visinelli, Weiqiang Yang, Alessandro Melchiorri, David F. Mota, Adam G. Riess, and Joseph Silk, “In the realm of the Hubble tension—a review of solutions,” *Class. Quant. Grav.* **38**, 153001 (2021), [arXiv:2103.01183 \[astro-ph.CO\]](#).
- [57] David Camarena and Valerio Marra, “On the use of the local prior on the absolute magnitude of Type Ia supernovae in cosmological inference,” *Mon. Not. Roy. Astron. Soc.* **504**, 5164–5171 (2021), [arXiv:2101.08641 \[astro-ph.CO\]](#).
- [58] George Efstathiou, “To H0 or not to H0?” *Mon. Not. Roy. Astron. Soc.* **505**, 3866–3872 (2021), [arXiv:2103.08723 \[astro-ph.CO\]](#).
- [59] Jesus Torrado and Antony Lewis, “Cobaya: Code for Bayesian Analysis of hierarchical physical models,” *JCAP* **05**, 057 (2021), [arXiv:2005.05290 \[astro-ph.IM\]](#).
- [60] Diego Blas, Julien Lesgourgues, and Thomas Tram, “The Cosmic Linear Anisotropy Solving System (CLASS) II: Approximation schemes,” *JCAP* **07**, 034 (2011), [arXiv:1104.2933 \[astro-ph.CO\]](#).
- [61] Antony Lewis, “GetDist: a Python package for analysing Monte Carlo samples,” (2019), [arXiv:1910.13970 \[astro-ph.IM\]](#).
- [62] Andrew Gelman and Donald B. Rubin, “Inference from Iterative Simulation Using Multiple Sequences,” *Statist. Sci.* **7**, 457–472 (1992).
- [63] Gen Ye, Bin Hu, and Yun-Song Piao, “Implication of the Hubble tension for the primordial Universe in light of recent cosmological data,” *Phys. Rev. D* **104**, 063510 (2021), [arXiv:2103.09729 \[astro-ph.CO\]](#).
- [64] Sunny Vagnozzi, “Consistency tests of Λ CDM from the early integrated Sachs-Wolfe effect: Implications for early-time new physics and the Hubble tension,” *Phys. Rev. D* **104**, 063524 (2021), [arXiv:2105.10425 \[astro-ph.CO\]](#).